



Article

Using a Microfluidics System to Reproducibly Synthesize Protein Nanoparticles: Factors Contributing to Size, Homogeneity, and Stability

Courtney van Ballegooie ^{1,2,*}, Alice Man ², Irene Andreu ^{1,3}, Byron D. Gates ³  and Donald Yapp ^{1,4,*} 

¹ Experimental Therapeutics, BC Cancer, Vancouver, BC V5Z 1L3, Canada; andreubirene@gmail.com

² Faculty of Medicine, University of British Columbia, Vancouver, BC V6T 1Z4, Canada; aliceman321@gmail.com

³ Department of Chemistry, Simon Fraser University, Burnaby, BC V5A 1S6, Canada; bgates@sfu.ca

⁴ Faculty of Pharmaceutical Sciences, University of British Columbia, Vancouver, BC V6T 1Z4, Canada

* Correspondence: cballegooie@bccrc.ca (C.v.B.); dyapp@bccrc.ca (D.Y.); Tel.: +1-604-675-8023 (D.Y.)

Received: 16 April 2019; Accepted: 9 May 2019; Published: 15 May 2019



Abstract: The synthesis of Zein nanoparticles (NPs) using conventional methods, such as emulsion solvent diffusion and emulsion solvent evaporation, is often unreliable in replicating particle size and polydispersity between batch-to-batch syntheses. We have systematically examined the parameters for reproducibly synthesizing Zein NPs using a Y-junction microfluidics chip with staggered herringbone micromixers. Our results indicate that the total flow rate of the fluidics system, relative flow rate of the aqueous and organic phase, concentration of the base material and solvent, and properties of the solvent influence the polydispersity and size of the NPs. Trends such as increasing the total flow rate and relative flow rate lead to a decrease in Zein NP size, while increasing the ethanol and Zein concentration lead to an increase in Zein NP size. The solvent property that was found to impact the size of the Zein NPs formed the most was their hydropathy. Solvents that had a hydropathy index most similar to that of Zein formed the smallest Zein NPs. Synthesis consistency was confirmed within and between sample batches. Stabilizing agents, such as sodium caseinate, Tween 80, and Pluronic F-68, were incorporated using the microfluidics system, necessary for in vitro and in vivo use, into Zein-based NPs.

Keywords: delivery systems; pharmaceuticals; zein nanoparticles; microfluidic coprecipitation; syringe pump

1. Introduction

Nanoparticle-based drug delivery systems have been investigated over the past few decades to improve the efficacy, bioavailability, and circulation half-life of small molecule drugs [1,2]. Modulating the particle's size and shape changes its biodistribution, and thus allows control over the pharmacokinetics of the loaded drug. In therapeutic applications for cancer, nanoparticles (NPs) <300 nm localize at tumor sites because they escape from leaky tumor vasculature in a process known as the enhanced permeability and retention effect (EPR) [2,3]. As tumor vessel pore cutoff sizes are typically between 380 and 780 nm, NPs between 100 and 300 nm can extravasate through the vessel pores into the perivascular area, and hence into the tumor microenvironment where the drug is eventually released [3]. The EPR effect, therefore, increases accumulation of the NP, and by extension, the loaded drug at the target site, and thus increases the drug's efficacy while decreasing its side effects [4].

NPs also play an important role in stabilizing poorly water soluble drugs in the bloodstream. Intravenous administration of anticancer drugs is a standard method for delivering chemotherapy and the stability and solubility of new pharmaceutical formulations is an important factor in their development. A classic strategy is to use formulation vehicles, such as oligomers of fatty acids or surfactant systems, to solubilize the drug. Unfortunately, some of these solubilizing vehicles, although approved for clinical use, have non-trivial toxicities. Cremophor EL (CrEL), a castor oil derivative used to solubilize paclitaxel, is associated with severe hypersensitivity reactions, hyperlipidemia, and peripheral neuropathy. NP colloidal systems can, thus, be used to avoid the problems associated with formulation vehicles, in addition to protecting the drug from premature degradation [5]. While stable drug plasma levels can be achieved through the gradual release of the drug from its carrier, burst doses of the drug can also be delivered to specific locations using external triggers, such as ultrasound or ionizing radiation [6,7]. Although NPs are promising for drug delivery in medical applications, issues such as their limited drug encapsulation efficiency, biocompatibility, and colloidal stability have thus far prevented their widespread use in the clinic [8].

Protein NPs, composed of multiple self-assembled protein subunits, are unique in that they can be highly biocompatible and contain a large number of reactive chemical groups for drug binding [9,10]. As the charge of their amino and carboxyl groups change in response to pH, protein NPs can be used for triggered drug release applications that are dependent on specific environmental conditions found in various compartments in the body, including the tumor microenvironment [11,12]. Proteins, particularly those from plants, are also bio-renewable, widely available, and have a broad range of isoelectric points [12–15]. The diversity of proteins, therefore, enables different drug classes to be matched with appropriate protein carriers to achieve maximal drug loading [12].

Nab-paclitaxel, a formulation of paclitaxel bound to human serum albumin (HSA) NPs, was the first protein NP successfully used in the clinic [16]. Albumin was used as an alternative for CrEL in the formulation of paclitaxel because of its low toxicity and preferential uptake by cancer cells [16,17]. Upon injection, *nab*-paclitaxel particles dissolve into albumin-paclitaxel complexes, allowing paclitaxel to bind with both injected and endogenous albumin. Although the formulation of *nab*-paclitaxel is in NP form, albumin is used as a vehicle rather than a drug carrier in the bloodstream due to its rapid dissociation into its protein subunits [16]. As a drug vehicle, the homogeneity of the albumin NP's size is of less importance for the formulation of *nab*-paclitaxel than it would be for other protein NPs used as drug carriers because of the dependence between NP size and pharmacokinetic properties [18].

Zein is a hydrophobic prolamin protein found in the endosperm of corn. This protein has generally recognized as safe (GRAS) status, is FDA-approved for specific applications in the pharmaceutical industry, and has an abundance of pre-clinical studies showing its potential for drug delivery [19]. The large number of hydrophobic residues present in the protein means that Zein NPs are suitable for sequestering hydrophobic drugs, and can be made using non-toxic solvents, such as ethanol (50% to 90%) and water [19,20]. Zein NPs would, therefore, be useful to encapsulate hydrophobic and toxic drugs, such as cisplatin or those found in the camptothecin family. The use of non-toxic solvent systems for preparing the drug-loaded NP is an additional advantage in the manufacturing process.

Coprecipitation, a particle formulation method based on a protein's differential solubility in two solvents, is commonly used to produce protein NPs, including Zein. This method is a benchtop process where an aqueous cosolvent is rapidly added to an organic phase solution of the protein to induce the precipitation of the protein in its NP form; the payload cargo is trapped within the matrix of the particle as it forms. The size of the particles produced depends on parameters, such as the ratio of the organic to aqueous phase, agitation speed, pH of the solution, and the flow rate of the aqueous phase into the organic [19–21]. Due to the spatial variation in the intensity of the shear forces within the solution, particle sizes vary and are inconsistent within batch-to-batch syntheses [22]. This variability becomes even more pronounced at larger scales and significantly hinders the scalability of the system. Thus, there is great interest in developing formulation methods that are easily modulated to produce

protein NPs of the desired size consistently from batch-to-batch, and which can be scaled up for mass production.

Microfluidic systems can be used to control the parameters affecting coprecipitation more rigorously and create NPs in a highly reproducible manner [23–25]. Aqueous and organic phases are still used in the same way to precipitate NPs, but microfluidic systems offer better control over the mixing at the junction where the two solvent streams meet. The laminar flow regime of the solvents and predictable flow patterns produce consistent mixing conditions that result in particles of uniform diameter [23]. To modulate the size and polydispersity of the NPs, parameters such as the relative flow rate of the aqueous and organic phase, the total flow rate of the fluidics system, and the properties of the solvents, can be adjusted. As opposed to conventional coprecipitation methods, microfluidic systems are scalable and show good potential for the production of NPs at industrial scales [26]. However, there are few systematic studies on the reproducibility of microfluidics for preparing protein NPs, and the system parameters that affect the size and polydispersity of the particles.

We report here the use of Y-channel microfluidic chips with staggered herringbone micromixers to synthesize Zein NPs reproducibly (Figure 1). The total flow rate of the fluidics system, the relative flow rate of the aqueous and organic phase within the fluidics system, the concentration of the reagents and protein, solvent properties, and the incorporation of stabilizers were systematically varied to ascertain their effects on the formation of Zein NPs. The results highlight the factors that affect the size of the NPs and batch-to-batch reproducibility when using microfluidics to synthesize Zein NPs.



Figure 1. A graphical depiction of the Zein nanoparticle (NP) synthesis using a coprecipitation microfluidics system. At the inlet channels, the organic phase is indicated in red while the aqueous phase is blue.

2. Materials and Methods

2.1. Materials

Zein from maize (Catalog number 9010-66-6), caesium sodium salt from bovine milk (Catalog number C8654), Acetonitrile (Catalog number 34998), Tween 20 (Catalog number 9005-64-5), and Tween 80 (Catalog number 9005-65-6) were purchased from Sigma-Aldrich (St. Louis, Missouri, USA). Isopropanol was purchased from Fisher Chemical (Catalog number PX1837/2). Ethyl alcohol anhydrous was purchased from Commercial Alcohols (Catalog number P016EAAN) and Pluronic F-68 (Catalog number 24040-032) was purchased from ThermoFisher Scientific (Waltham, Massachusetts, USA). Reagents were used as received, unless otherwise stated. Acrodisc syringe filters (13 mm, 0.8 μ m

membrane) were purchased from Pall (Show Low, AZ, USA). Slip tip syringes for 3 (Catalog number 309586), 1 (Catalog number 309659), and 10 (Catalog number 309604) mL volumes were purchased from Becton Dickinson (Mississauga, Ontario, Canada). Conical centrifuge tubes of 50 (Cat. 352070) and 15 (Catalog number 352196) mL volume were purchased from Fisher Scientific (Toronto, Ontario, Canada). A Float-A-Lyzer G2 dialysis device (molecular weight cut-off 100 kDa) was purchased from Spectrum Labs (Catalog number 6235035, Boston, MA, USA). Zein NPs were synthesized using a Benchtop NanoAssemblr (Precision Nanosystems, Vancouver, British Columbia, Canada) or a combination of a MEDFUSION (Smiths Medical, Dublin, OH, USA) and New Era NE-1000 syringe pump (New Era Pump Systems, Farmingdale, NY, USA). Samples were analyzed using a NanoBrook ZetaPALS (Brookhaven Instruments, Long Island, OH, USA). Ultraviolet-Visible Spectroscopy (UV-Vis) was performed on a Nanodrop Spectrophotometer ND-1000. Centrifugation was performed on an Eppendorf Centrifuge 54150 (Mississauga, Ontario, Canada). using Eppendorf tubes (VWR, Radnor, Pennsylvania, USA, Cat 20170-577). Scanning electron microscopy (SEM) was performed using a FEI Nova NanoSEM (FEI, Hillsboro, Oregon, USA) with samples being prepared on a 300-mesh formvar/carbon-coated copper grid (Catalog number FCF-300; supplier Electron Microscopy Sciences, Hatfield, PA, USA).

2.2. Zein NP Microfluidics Synthesis

Zein (0.05–0.20 g) was dissolved in 10 mL of ethanol, acetonitrile, or isopropanol in a 50 mL falcon tube and stirred at 400 RPM for 3 h. Subsequently, the Zein solution was filtered through a 13 mm syringe filter (0.8 μ m). The filtered Zein solution was loaded into a syringe (1.0 mL) as the organic phase in the first inlet channel while its counterpart aqueous phase was loaded into a 3.0 mL syringe in the second inlet channel (Figure A5). The sample was run at various total flow rates (TFR) and relative flow rates (RFR) and collected at the microfluidics chip's outlet channel. Each run was programmed to discard the first 0.3 mL of the sample and the last 0.1 mL of the sample to ensure that the variability in fluid dynamics at the start and end of the synthesis run did not affect the sample. Samples (0.5 mL) were transferred to 1.5 mL Eppendorf tubes, centrifuged (1000 g; 10 min), and the precipitate was kept at room temperature for 1 h before analysis.

2.3. Zein NP Batch Synthesis

This synthesis was adapted from Baars et al. [27]. Briefly, Zein NPs were prepared by a coprecipitation method. A stock solution was made by dissolving Zein (1.0 g) in 40 mL of 80:20 ethanol-water solution in a 50 mL falcon tube. The solution was stirred at 400 revolutions per minute (RPM) until the Zein was dissolved (approximately 3 h). Subsequently, the solution was poured slowly into 120 mL of 18.0 M Ω milli-Q water with constant stirring (400 RPM), resulting in a yellow turbid dispersion of Zein NPs. The suspension of Zein NPs was stirred for 10 min after the complete addition of the Zein before collection and analysis.

2.4. Zein NP Syringe Pump Synthesis

The Zein solution was prepared as described in Section 2.3; the Zein solution was loaded into a syringe (10 mL) and secured into the first syringe pump. The desired aqueous phase was also loaded into a syringe (10 mL) and placed into a second pump. Both syringe pumps were then connected to 15 cm of 1/32" diameter vinyl tubing and fitted to a polyvinyl T- or Y- junction. The outlet was subsequently connected to 140 cm of the same tubing. The desired flow rates were set on the syringe pumps and solvent flows activated simultaneously. The first mL was discarded, and the subsequent 0.5 mL of the sample was collected in a centrifuge tube. The collected samples were centrifuged (1000 g for 10 min) at room temperature and set aside for 1 h prior to analysis.

2.5. Zein Purification

Zein purification was adapted from De Boer et al. [28]. Zein (0.10 g) was suspended in 15 mL of anhydrous ethanol. The suspension of proteins was stirred overnight (400 RPM at 4 °C). The following

day, stirring was stopped, and the insoluble Zein was allowed to settle. The supernatant containing impurities was removed, and the collected Zein was resuspended in anhydrous ethanol again. This process was repeated for a total of two to three times with the desired solvent used in the final hydration step. Purified Zein, also known as white Zein, was then used in the same manner as the unpurified Zein in the NP synthesis steps.

2.6. Stabilizer Preparation

Sodium Caseinate (SC)–SC (0.30 g) was dissolved in 10 mL of milli-Q water and stirred at 400 RPM for 3 h. This stock solution was diluted to the appropriate concentrations (0.25, 0.50, 0.75, 1.00, and 2.00% *w/v*) with milli-Q water. SC was used as the aqueous phase in the presence and absence of Zein in the organic phase, which contained 60% ethanol. Tween 20 (TW20)–A 1.00% (*v/v*) TW20 stock was made by diluting TW20 in milli-Q water. This stock was then diluted to the appropriate concentrations (0.25, 0.50, and 0.75% *v/v*). The diluted stocks were heated in a water bath (45 °C for 45 min) and cooled to room temperature before use. TW20 samples were used as the aqueous phase when using microfluidics in the presence of Zein in the organic phase, which contained 60% ethanol. Tween 80 (TW80) and Pluronic F-68 (F-68)–A 10.00% (*v/v*) F-68 and 2.00% (*v/v*) TW80 stock were used to make the following multi-component samples: 0.05% TW80 and 1.00% F-68; 0.50% TW80 and 1.00% F-68; and 1.00% TW80 and 1.00% F-68. Each solution mixture was then heated in a water bath (45 °C for 45 min) and cooled to room temperature before use. TW80 and F-68 samples were used as the aqueous phase and Zein was present in the organic phase (60% ethanol) in the microfluidic system.

2.7. Stabilized Zein Purification

The dialysis tubing was activated as described by the manufacturer. Briefly, the tube was rinsed in 10% ethanol for 10 min followed by a 20-min rinse with deionized (DI) water. Subsequently, stabilized Zein NP was added to the interior of the tubing (0.5 mL). The sample was then dialyzed against a 1000 mL milli-Q water bath that was stirred at 200 RPM at 4 °C. The water bath was changed at 12 h intervals for a total of 2 times. Each time the water bath was changed, a sample (7 µL) was removed from the dialysis tubing for analysis by dynamic light scattering (DLS) and UV-Vis spectroscopy.

2.8. Zein Scanning Electron Microscopy (SEM) Preparation

Zein samples were diluted 10 times in milli-Q water (100 µL of sample + 900 µL of water) in an Eppendorf tube immediately prior to sample preparation. The sample (3–5 µL) was spotted on the copper grid and dried under reduced pressure (1–2 h). The samples were imaged immediately after using a SEM FEI Nova NanoSEM (5 kV and 20 kV acceleration voltage, secondary electrons, and backscattered electrons, as well as immersion mode).

2.9. Statistics and Image Processing

Data were reported as the average mean with the error bars representing the standard deviation (SD) for triplicate determinations. One-way ANOVA and Tukey's tests were employed to identify differences in means. Statistics were analyzed using Graph Pad Prism 7. Statistical significance was declared at the following levels: * $p < 0.05$, ** $p < 0.01$, *** $p < 0.001$, and **** $p < 0.0001$. When no statistical significance was identified, it was indicated as ns above each sample condition. Image processing to verify Zein NP size was performed on SEM images using ImageJ. The SD of the SEM values was found to be 75.6 nm.

3. Results and Discussion

3.1. Formulation Factors and Reproducibility

Zein NPs form according to the basic principles of a liquid–liquid dispersion (LLD) process; the soluble phase (ethanol) containing Zein is introduced to the bulk insoluble phase (water). When

these phases are introduced in the presence of mixing, shearing forces cause small droplets of ethanol-Zein to form. The ethanol contained within the droplet is then able to partition into the bulk water, termed solvent attrition, due to the miscibility of ethanol and water. Once solvent attrition occurs, and ethanol concentrations decrease below the solubility limit of Zein, the protein precipitates and forms NPs [19]. During LLD, there are three competing mechanisms that influence particle formation. First, shear forces break the soluble phase into droplets. Second, the particle begins the process of precipitation [19,29]. At this point in time, the saturation of the system will determine the number of initial nuclei formed as given by the primary nucleation equation Equation (1):

$$J \propto \exp(-16\pi\gamma^3 v^2 / 3k^3 T^3 (\ln S)^2) \quad (1)$$

$$S = c(r)/c^* \quad (2)$$

$$\ln(S) = 2\gamma/rTk \quad (3)$$

where γ is the solid–liquid interfacial tension, v is the molar volume, k is the Boltzmann constant, and T is the temperature. The rate of nucleation is coupled with the particle radius and supersaturation (Equation (2)), and through the Ostwald–Freundlich equation (Equation (3)), where $c(r)$ denotes the solubility of a particle with radius r , and c^* is the equilibrium [29]. If the transition between nucleation and discrete particle formation is prolonged, a mechanism termed Ostwald ripening (OR) can occur, where smaller NPs can dissolve and combine with larger particles, since the concentration has dropped below the saturation concentration for droplets of their size [19,30]. This process can occur in seconds or minutes and results in larger and less-polydisperse samples. The third mechanism is the coalescence of the particles within the system. Coalescence can occur if the ethanol concentration within the droplet is sufficiently high enough to solubilize Zein when two particles interact with each other due to shearing or Brownian motion. If the particle fully precipitates while coalescence is occurring, large or irregular structures may be produced. However, if the nuclei cease to interact or if there is no interaction to start with, discrete Zein NPs may be formed [19].

Although the three competing mechanisms also occur in the microfluidics process, the impact of each mechanism on particle formation will change relative to that seen in LLD [31]. In the present study, extrinsic and intrinsic parameters of the microfluidic system are examined and compared to its LLD counterpart. In order to study the effect of each parameter on NP formation, our group determined changes in the Zein NP size (measured as the diameter) and polydispersity (PD) as one parameter was varied. Changes in NP size and PD were compared to a standard group of particles made with 1.00% *w/v* Zein stock solution, an ethanol concentration 60% *v/v*, a relative flow rate (aqueous to organic phase) fixed at 3 to 1, and a total flow rate of 2.00 mL/minutes (mL/min). Each parameter was then modulated systematically and its effect on particle size and PD were evaluated. The control or standard Zein particles are shown as purple points within each graph, and comparative statistics were carried out between each experimental sample and the control, standard group.

3.1.1. Effect of TFR and RFR on Zein NP Size and PD

The effects of total flow rate (TFR) and relative flow rate (organic to aqueous phase ratio, RFR) in the Y-junction microfluidic synthesis were investigated. The results shown in Figure 2a indicate that the NPs produced were significantly smaller when the total flow rate was increased (70.65 nm; 8.00 mL/min; $p < 0.001$), and significantly larger when the total flow rate was decreased (99.95 nm; 0.25 mL/min; $p < 0.01$). There was, however, no observable decrease in particle size when increasing the flow rate from 6.00 mL/min to 8.00 mL/min. Overall, a higher (relative to the control) total flow rate decreases the size of the droplet formed during the breakup of the soluble phase, and therefore, the number of nuclei that can be formed within the droplet. The decreased number of nuclei within each droplet results in the decrease in the average final particle size [29,32]. Similar findings have been seen in both LLD and T- and flow focused microfluidics configurations [19,31].

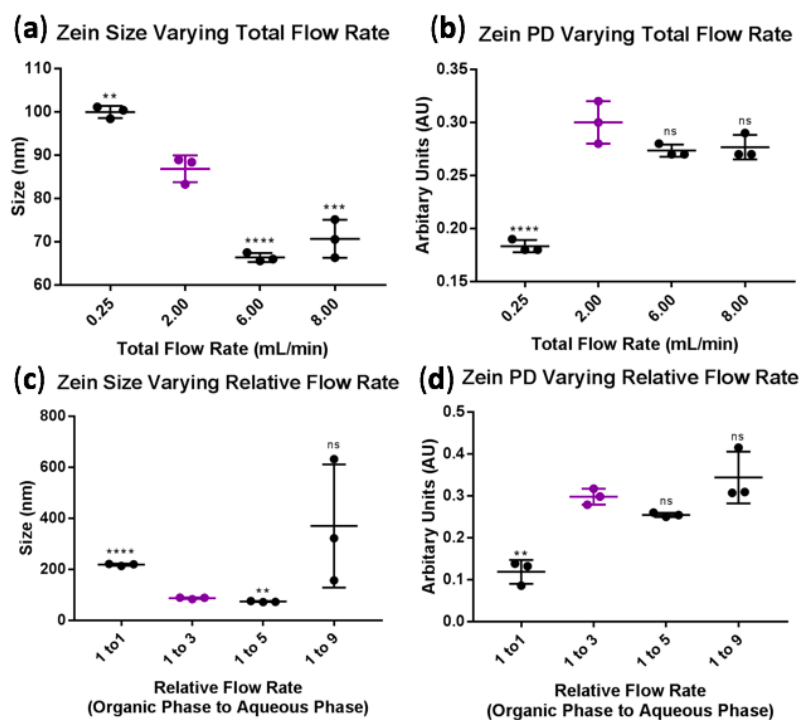


Figure 2. Changes in Zein nanoparticle (NP) diameter synthesized in the microfluidic Y junction as a function of: (a) Total Flow Rate (TFR); (c) Relative Flow Rate (RFR). Changes in Zein NP polydispersity (PD) as a function of: (b) TFR; (d) RFR.

Increasing the RFR (1:5; Figure 2c) significantly reduces the size of the NP produced (73.44 nm; $p < 0.01$), but when the RFR is reduced to 1:1, the NP's sizes increase significantly (218.01 nm; $p < 0.0001$). These changes observed at a RFR of 1:5 and lower occur because the increase in aqueous flow rate creates a situation where there are higher instances of supersaturation of the solute, which in turn increases the number of nuclei formed and ultimately decreases the average size of the final particles formed. The reverse situation results in the formation of larger particles. The decrease in diameter with increasing relative flow rate has been seen previously in LLD by Zhong and Jin [19]. The PD in the samples containing a TFR of 0.25 mL/min or an RFR of 1:1, as seen in Figure 2b,d, likely decreased due to the increased time available for Zein to solidify; an increased attrition time would allow more time for small Zein nuclei to undergo OR, thereby potentially narrowing the size distribution. This hypothesis was similarly demonstrated using a flow focused and T-junction microfluidics configuration [19,31].

In a microfluidic reactor, particle formation relies mainly on the diffusion of the ethanol from the organic phase (dispersed phase) to the aqueous phase (continuous phase). This concept holds true when using low ratios of relative velocities between the organic and aqueous phases, as discussed previously. However, when a high RFR (1:9) was used with the microfluidic system described here, a high PD and incident of particle deformation were observed. While this result was surprising, we attribute the deformation, and an associated increase in PD, to the different spatial shearing intensities that occur at high (versus lower) RFRs. At RFRs of 1:5 and lower, the diffusion of ethanol into the aqueous phase is the dominant mechanism, with shear rates playing a smaller role in particle formation. However, at a RFR of 1:9 the shear rates may have a larger effect on the droplet and particle formation process. We expect that the organic phase closest to the wall of the microfluidic channel will experience the greatest shear forces rates relative to those at the center of the channel. The variation in shear forces, therefore, leads to different rates of particle nucleation within the system. For example, if the droplet formed at a point located near the aqueous phase, supersaturation conditions would lead to a large number of small particle nuclei. In contrast, if droplet formation occurred closest to the wall of the

microfluidic system, the higher concentration of ethanol (due to it being located further away from the aqueous phase) would cause a delay in discrete particle formation, thereby resulting in larger nuclei, increased coalescence, and even potentially particle deformation. Although this phenomenon was not seen in Zein particles using a flow-focused or T-junction microfluidics configuration, it is likely that the different fluid dynamics due to the configuration of the microfluidics chips, as well as the magnitude in the difference between the two phases, influenced shear stress [31].

3.1.2. Effect of Ethanol Concentration on Zein NP Size and PD

Figure 3a shows the changes in Zein NP size when the concentration of ethanol is changed. No significant changes in size (compared to control NPs used with 60% ethanol) were seen up to 80% ethanol; however, at an ethanol concentration of 90%, NP sizes increased significantly (81.12 nm and 108.86 nm for 60% and 90% ethanol respectively; $p < 0.001$). These data suggest a positive correlation exists between increasing ethanol concentration and the size of the NP formed. The observed increase in NP size likely occurs because of OR; the higher concentrations of ethanol require more time to partition out of the droplet, thereby increasing the time for Zein to precipitate and undergo OR. The PDI would, therefore, be expected to decrease under these conditions, which is indeed the case (Figure 3b, $p < 0.0001$).

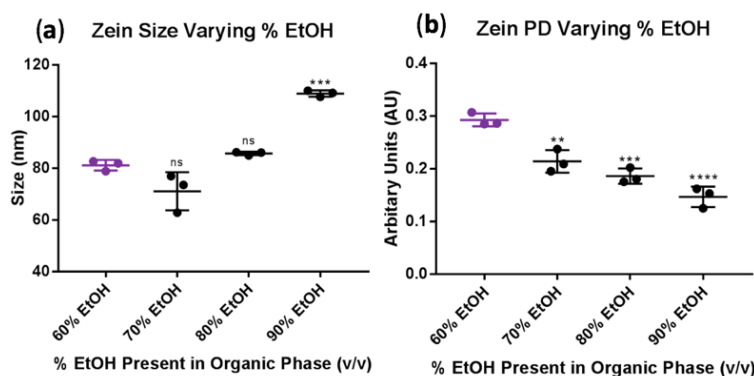


Figure 3. Impact of the percentage of ethanol present on Zein nanoparticles (NPs): (a) diameter; (b) polydispersity (PD).

While this finding has been confirmed in other microfluidics configurations, such as flow focused and T-junction, in LLD a decrease in NP size with increasing ethanol concentration was observed [31]. It was hypothesized that the increased ethanol concentration would allow more time for coalesced Zein to be sheared into smaller particles before solidifying [19,31,33]. However, due to the reduced shear found in the microfluidics systems, this increase in attrition time may have allowed for increased coalescence and OR, and, therefore, larger NP diameter.

3.1.3. Effect of Zein Concentration on Zein NP Size and PD

The effects of the Zein concentrations on NP size can be seen in Figure 4a; the size of the NPs produced was significantly smaller with a Zein concentration of 0.50% w/v ($p < 0.001$), but particle size increased significantly at Zein concentrations of 2% w/v ($p < 0.01$). In Figure 4b, the PD significantly decreased with increasing Zein concentration ($p < 0.0001$). Increasing the Zein concentration increases the viscosity of the solution, which reduces the diffusivity of the solvent, as represented by Stokes-Einstein diffusivity equation:

$$D = (k_B T)/(6\pi\eta r) \quad (4)$$

where k_B is Boltzmann's constant, T is absolute temperature, η is dynamic viscosity, and r is the radius of the molecule [31,34]. The observed increase in NP size with increasing Zein concentration, therefore,

occurs due to the decreased diffusivity of ethanol within the droplet, and, therefore, increased growth via OR, in addition to the increased density (droplets/mm³) of nuclei formed within the droplet.

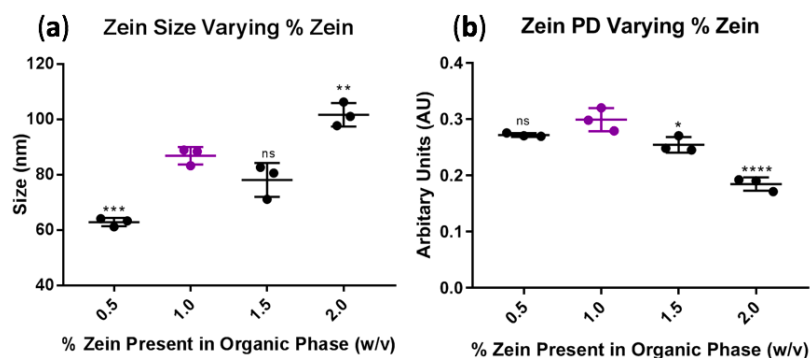


Figure 4. Impact of the percentage of Zein present on Zein nanoparticles (NPs): (a) diameter; (b) polydispersity (PD).

The positive correlation between Zein concentration and NP size was also reported in a previous study using the LLD method, where the viscosity of the dispersed phase increased with increasing Zein concentrations [18]. Higher solvent viscosity would slow down the deformation of droplets under shear, leading to the formation of NPs with a larger size. Compared to the LLD method, the microfluidic process involves much less shear, and consequently, the deformation of droplets becomes negligible, while the diffusion of ethanol from the dispersed phase to the continuous phase is of greater significance. The results shown in Figure 3e suggest that PD was most greatly influenced by the diffusivity of the system, and therefore increased OR, and lead to a decreased PD in instances of higher Zein concentration [31].

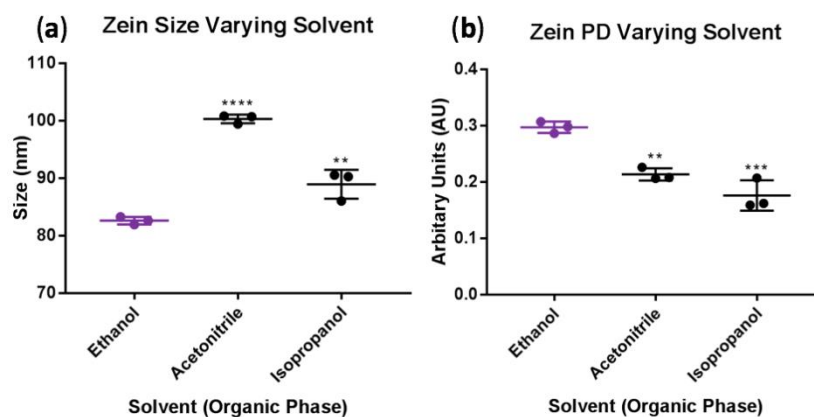
3.1.4. Effect of Solvent Type on Zein NP Size and PD

The observed change in Zein NP sizes, when used with different solvents, depends on the solvent's polarity. The hydrophathy index of Zein's major constituents (Z19 and Z22), which comprise approximately 80% of the protein, is 4.70 and 4.86, respectively [35,36]. The hydrophilicity of the solvents is indicated in Table 1. Under the basic principles of "like dissolves like", we would then expect that Zein is most soluble in ethanol, and least soluble in acetonitrile. The differences in the solubility of Zein in different solvent mixtures result in different supersaturation levels during nucleation. Ethanol would create higher supersaturation levels after the introduction of water. The increased supersaturation level increases the number of nuclei formed, which in turn decreases the average size of the final particles. The solvent's polarity seems to be the system's driving factor in NP formation, as indicated by Figure 5a. Similar findings were experimentally validated in LLD by Vitale and Katz, where they demonstrated that divinyl benzene formed smaller particles in ethanol than acetonitrile, despite the differences in the solvents' viscosities and diffusion coefficients [30]. It should be noted that in an LLD by Patel et al., isopropanol was found to produce smaller Zein particles than ethanol. However, in this report, the range of sizes had significant overlap with the deviation of the mean and no statistical analysis was performed to indicate whether the difference was significant [29].

When discussing the PD, it is likely that the larger droplets formed quickly and discretely in acetonitrile, due to its low viscosity, quick diffusion, and affinity for water (Log K_{OW}), as seen in Table 1. The PD of particles in isopropanol likely decreased due to its diffusion coefficient and viscosity, which would result in an increase in OR.

Table 1. Density, Viscosity, Hydropathy Index, Log K_{ow}, and Diffusion Coefficients for the Solvents.

	Density (g/mL) at 20 °C	Viscosity (cP) at 20 °C	Hydropathy Index (Arbitrary Units)	Log K _{ow}	Binary Liquid Diffusion Coefficient in Water ($\times 10^{-5}$ cm ² /s) at 25 °C for 0.50 c/(mol dm ⁻³)
Ethanol	0.79 [37]	1.22 [37]	5.2 [36,38]	−0.16 [38]	1.14 [39]
Acetonitrile	0.79 [37]	0.35 [37]	5.8 [38]	−0.17 ¹ [38]	2.40 [40]
Isopropanol	0.79 [37]	2.37 [37]	3.9 [38]	0.25 [38]	0.92 [39]

¹ Expected value of −0.34 [38].**Figure 5.** Impact of the solvent type on Zein nanoparticles (NPs): (a) diameter; (b) polydispersity (PD).

3.1.5. Batch to Batch Consistency

Proteins have many attractive qualities as a NP drug delivery system; however, controlling their particle size and minimizing batch-to-batch variations during their synthesis is difficult [41]. Therefore, in order to circumvent this disadvantage, a Y-channel microfluidics reactor was chosen for both its herringbone structures, for increased laminar flow, as well as the system's overall tunability and scalability. The previous sections in this report demonstrate the tunability of the system; however, we also evaluated the variation between batches of Zein NPs made using the same formulation parameters (TFR 2 mL/min, RFR 3:1, 1% *w/v* Zein in 60% *v/v* ethanol) over a period of several weeks. The diameters and PDs of the different Zein NP batches made were found to be consistent, as shown in Figure 6a,b, respectively.

Confirmation of the DLS data was established using scanning electron microscopy (SEM; Figure 6c,d). Although the histogram demonstrates that most of the NPs are distributed near the mean of the DLS data, it can be seen that larger particles (>300 nm) are also present. The presence of large NPs was not observed in the DLS analysis (data not shown), and the apparent discrepancy between DLS and SEM data is likely an artifact of sample preparation for SEM. During the preparation the sample is dried under vacuum; since these NPs are not stabilized with surfactants, the particles come into proximity and can merge to form aggregates [42,43]. These extreme size values generated by the aggregated Zein NPs is reflected in the calculated SD of the sample (75.6 nm). Regardless, the distribution calculated from the NPs imaged using SEM, when aggregation was taken into consideration, correlated well to the data obtained by DLS, thereby further validating the data obtained by DLS.

The consistency data, obtained using the Y-channel microfluidics reactor, were compared to data obtained using other synthesis methods, such as the batch and syringe pump synthesis. A similar set of parameters were tested on a larger Y-junction dual syringe pump system (TFR 6 mL/min, RFR 3:1, 1% Zein in 60% ethanol) over a period of several weeks. As shown in Figure A3a,b (Appendix A), significant differences in the diameter and PD of the Zein NPs were detected across the 12 trials, with some trials producing NPs that varied by over 100 nm in size. Modifications to the system, such as

adjusting the RFR to 5:1 (Figure A3e,f), adding stabilizers (0.5% *v/v* Tween 80 and 1% *w/v* Pluronic F-68) to the aqueous phase (Figure A3c,d), or use of a T-junction, did not improve the batch-to-batch variation (Figure A3k,l). A coprecipitation batch synthesis method was also tested, showing significant differences in size and polydispersity of NPs between trials ($p < 0.0001$). While all other datasets shown have the points on the graph representing discrete batches, the batch synthesis was comprised of multiple measures of the same trials ($n = 2$). This was done in order to not only visualize between trial variability but also within trial variability as well. Overall, the batch and syringe pump synthesis suggest that other methods, such as the Y-channel microfluidics chip, should be pursued in order to synthesize tunable and reproducible protein NPs.

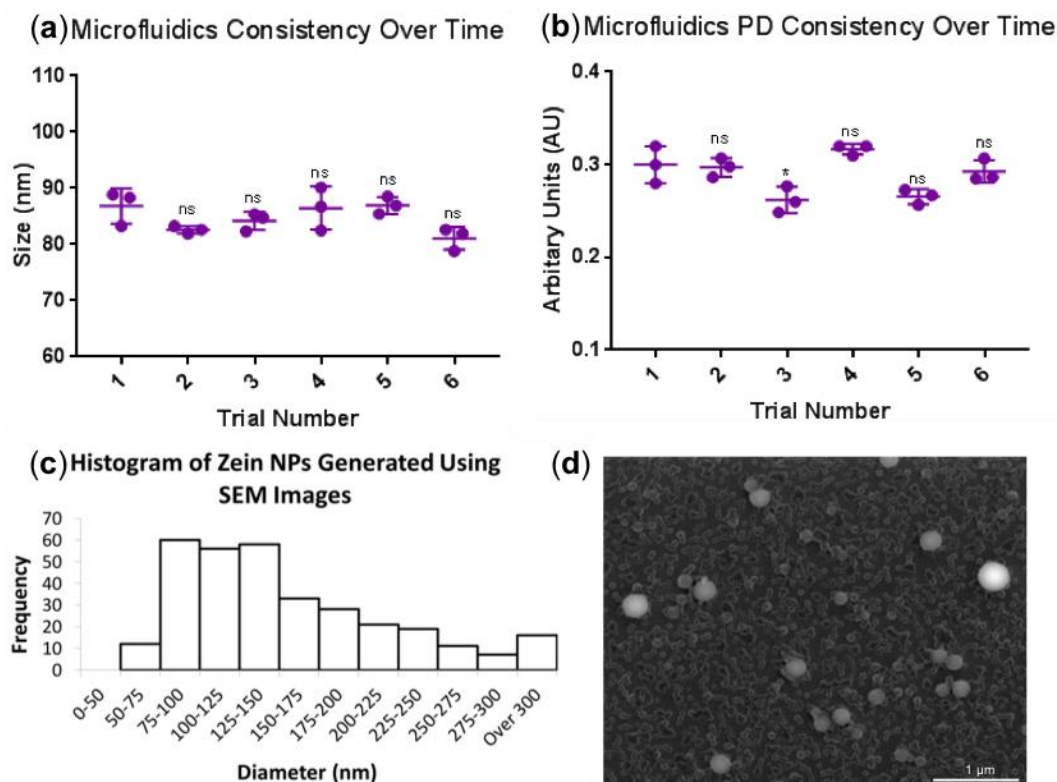


Figure 6. Reproducibility of Zein nanoparticles (NPs) made using a microfluidics system as demonstrated by: (a) the diameter of Zein NPs produced with the same parameters using different stocks on different days; (b) the polydispersity (PD) of Zein NPs produced with the same parameters using different stocks on different days; (c) a histogram of a Zein NP sample generated using scanning electron microscopy (SEM) images that was determined to be 113 nm using dynamic light scattering (DLS); (d) a representative SEM image of the 113 nm sample obtained.

3.2. Functionality and Stability

Once the microfluidics system was confirmed to be both a tunable and consistent method for forming Zein NPs, stabilizing methods were then investigated. Stabilizers Sodium Caseinate (SC) and Tween-80 (TW80) with Pluronic F-68 (F-68) were chosen due to their use in *in vivo* and *in vitro* experimentation [44–46].

SC, as a Zein NP colloidal stabilizer, was first introduced by Patel et al. in 2010 for oral delivery applications. SC was chosen as a stabilizer due to the electrostatic interactions of the negatively-charged SC with Zein, as well as the steric hindrance it provides. In their experiments, they saw that using SC with Zein in an LLD resulted in 120–150 nm negatively-charged particles that had a shifted isoelectric point (from pH 6 to 5). This finding was significant, as it suggested that the NPs would be stable at the biological pH of 6.2 [29]. Lou et al. later explored this theory, where they tested the stability of the SC-Zein particles in Hank's Balanced Salt Solution-4-(2-hydroxyethyl)-1-piperazineethanesulfonic acid

(HBSS-HEPES) and Dulbecco's Modified Eagle's medium (DMEM) [44]. The particles, depending on their SC:Zein ratio, were stable and showed minimal to no change in size in most of the experimental conditions. Cell toxicity and uptake were then explored and demonstrated minimal toxicity and increased uptake when using higher ratios of SC:Zein. Based on these findings, as well as the ability of the SC-Zein system to encapsulate hydrophobic compounds, SC made an attractive candidate for the microfluidics system. Interestingly, in these experiments, the size of the SC-Zein NP seemed to increase only minimally with increasing SC concentrations (Figure 7a). These findings are consistent with the LLD method, suggesting that the different forces and increased homogeneous mixing found in the microfluidics chip had no impact on the interactions between SC and Zein. This was further reinforced, as the small drop in PD when using 1% SC was also prevalent in the LLD method [14,29]. From these experiments, it can be seen that the Y-channel microfluidics chip can be used to create SC-Zein NPs comparable to that of the LLD method.

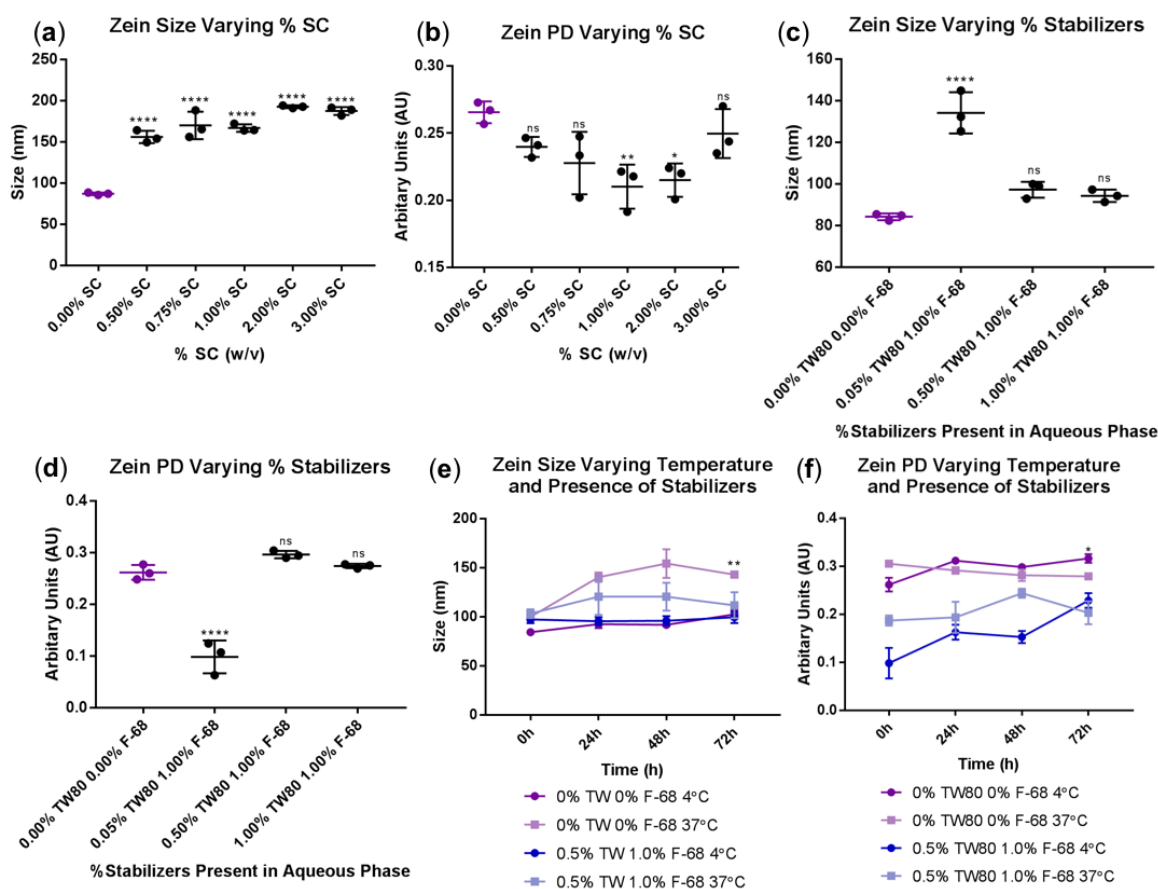


Figure 7. The ability to functionalize Zein nanoparticles (NPs) using a microfluidics system as demonstrated by: (a) the diameter of Zein NPs' varying% of sodium caseinate (SC); (b) the polydispersity (PD) of Zein NPs' varying% SC; (c) the diameter of Zein NPs' varying% of stabilizers; (d) the PD of Zein NPs' varying% stabilizers; (e) the diameter of Zein NPs' varying temperatures and presence of stabilizers; and (f) the PD of Zein NPs' varying temperatures and presence of stabilizers.

A variety of amphipathic surfactants (e.g., polysorbates such as Tween 80, Tween 20, etc.) and lipids (phospholipids, glycerophospholipids, etc.) have been used in combination with Zein. In theory, the non-polar tails of the amphipathic surfactants will adsorb on the non-polar areas of the Zein protein. The colloidal stability is then improved due to the steric hindrance provided by the polar head group [42,43]. However, if these surfactants are used as a single stabilizing agent, partial unfolding of the Zein will occur and the protein NPs themselves will be destabilized, as seen by Mahal et al., and as demonstrated here using Tween 20 (Figure A1a) [47]. Therefore, poloxamers-triblock copolymers with

a central hydrophobic chain of polyoxypropylene and two hydrophilic chains of polyoxyethylene are used in conjunction with amphipathic surfactants. The concentrations and compositions of the surfactants were based on the *in vivo* formulation of Jain et al. and modulated using the findings of Podaralla and Perumal [45,48]. Our findings were similar to those reported by Podaralla and Perumal when modulating the concentrations of TW80 when in the presence of F-68. Briefly, concentrations of TW80 below 0.5% lead to larger particles and aggregates, as indicated by the larger size distribution between the batch-to-batch replicates, while samples containing 0.5% or greater concentrations of TW80 and F-68 led to small, stable particles. It should be noted that formulations containing F-68 concentrations lower than those of TW80 were not studied due to their already well documented instability and lack of pre-clinical applications [45–49].

Once formulations of TW80 and F-68 stabilized Zein NPs were synthesized, the resulting NPs were dialyzed to remove the excess TW80 and F-68, as shown in Figure A2. NPs that were dialyzed and stabilized, as well as NPs that contained no stabilizers, were incubated at both 4 °C and 37 °C. It has been shown previously that Zein NPs can increase in size, either by swelling or aggregating, at elevated temperatures [42,43]. The protein's swelling and aggregating, however, can be mitigated by stabilizing the protein NPs [43,46]. Indeed, as seen in Figure 7e, only NPs that were incubated at 37 °C and not stabilized increased in size over the course of 72 h relative to their 4 °C counterpart. This finding suggests that Zein NPs were stabilized by TW80 and F-68 when synthesized using the microfluidic device.

4. Conclusions

A tunable and reproducible method for Zein NP synthesis was established using a Y-junction microfluidics system. The modification of the total flow rate of the fluidics system, relative flow rate of the aqueous and organic phase, and concentration of the base material and solvent allowed for Zein NP size and PD to be controlled. The reproducibility of the synthesis method was shown through the formation of Zein NPs with consistent sizes and PD over six trials. The stabilizer TW80 with F-68 was found to increase Zein NPs stability over time. Overall, the Y-junction microfluidics formulation technique shows promise in creating tunable and reproducible protein NPs that can be used to encapsulate drugs for future *in vitro* and *in vivo* applications. Having established a reproducible method of synthesizing stabilized Zein NPs, our group will further extend these studies by loading other materials (e.g., drugs or gold NPs) into the Zein NPs.

Author Contributions: Conceptualization, C.v.B.; methodology, C.v.B. and I.A.; formal analysis, C.v.B.; investigation, C.v.B. and A.M.; resources, B.G. and D.Y.; writing—original draft preparation, C.v.B. and A.M.; writing—review and editing, C.v.B., I.A., B.G., and D.Y.; visualization, C.v.B.; supervision, B.G. and D.Y.; funding acquisition, C.v.B., B.G., and D.Y.

Funding: This research was funded by the Canadian Institutes of Health and the National Sciences and Engineering combined program (CHRP). C.v.B. was funded by a Canadian Graduate Scholarships-Master's Program, Canadian Institutes of Health Research (CGS-M CIHR) and a University of British Columbia Graduate Fellowship.

Acknowledgments: The authors would like to thank and acknowledge Alessia Pallaoro's and Marcel Bally's contributions, including the use of the NanoAssemblr device.

Conflicts of Interest: The authors declare no conflict of interest.

Appendix A

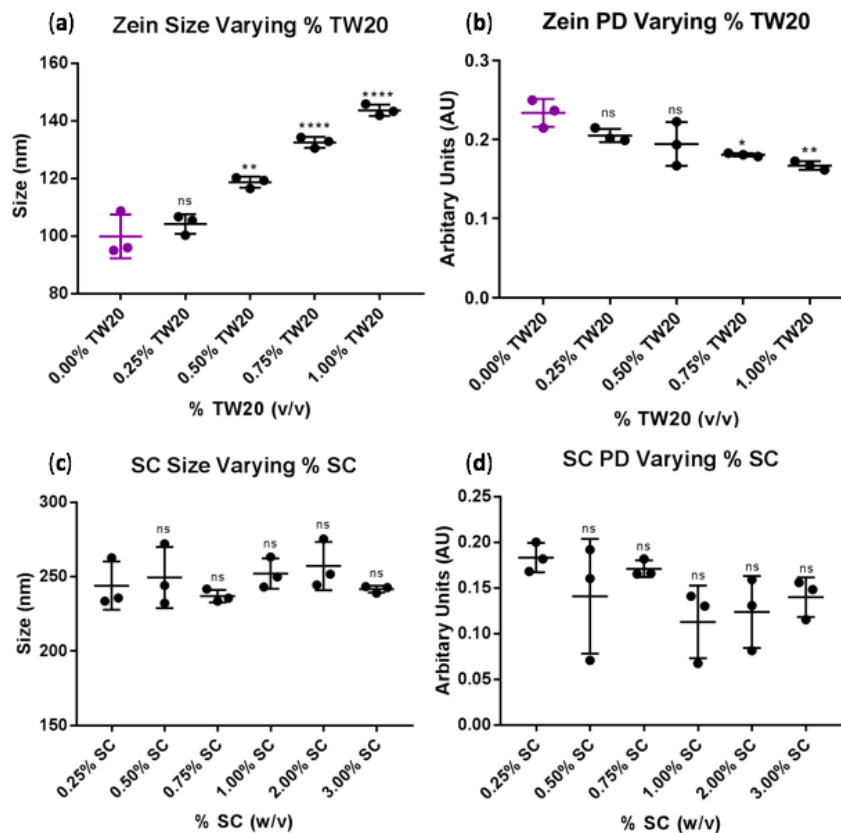


Figure A1. (a) The diameter of Zein nanoparticles (NPs) varying % Tween 20 (TW20); (b) the polydispersity (PD) of Zein NPs varying % TW20; (c) the diameter of sodium caseinate (SC) varying % SC when produced using the standard microfluidics conditions of Zein; (d) the PD of SC varying % SC when produced using the standard microfluidics conditions of Zein.

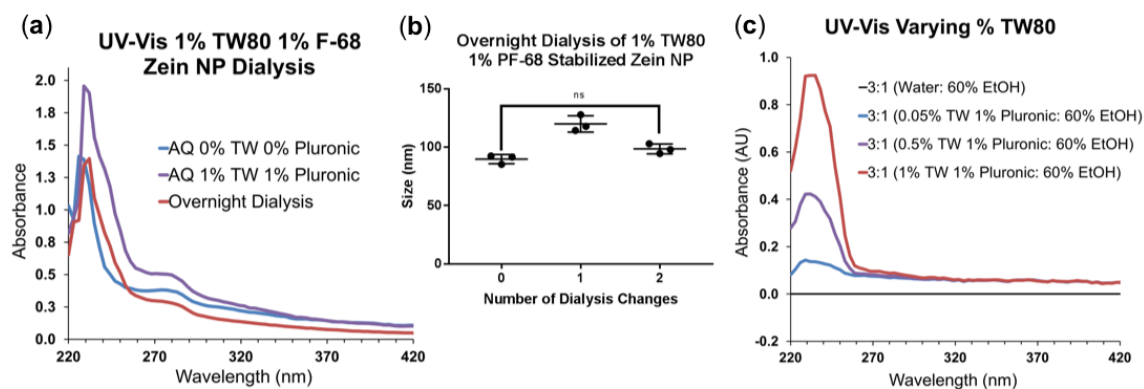


Figure A2. Removing excess stabilizers not incorporated in Zein nanoparticles (NPs): (a) Ultraviolet-Visible Spectroscopy (UV-Vis) of the 1% Tween 80 (TW80) 1% Pluronic F-68 (PF-68) NP before and after dialysis with control sample containing no stabilizers for reference; (b) the change in size of the 1% TW80 1% PF-68 at each dialysis change; and (c) UV-Vis of the TW80 present in each of the Zein NP samples with stabilizers.

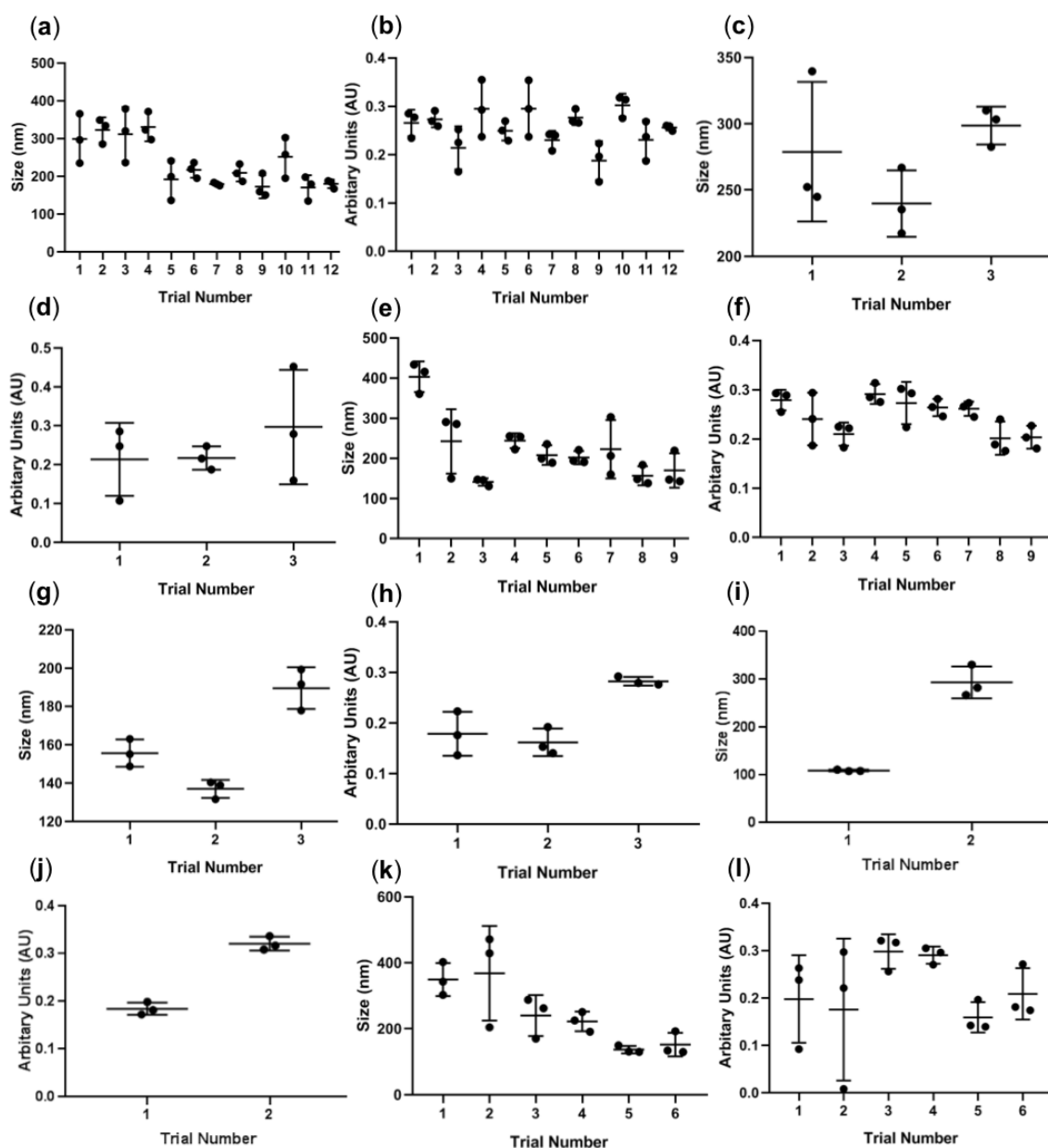


Figure A3. The batch-to-batch consistency between trials: (a) the diameter of Zein nanoparticles (NPs) using a syringe pump synthesis under standard conditions, $n = 36$; (b) the polydispersity (PD) of Zein NPs using a syringe pump synthesis under standard conditions, $n = 36$; (c) the diameter of Zein NPs using a syringe pump synthesis under standard conditions with stabilizers [0.5% Tween 80 (TW80) 1.0% Pluronic F-68 (PF-68)], $n = 9$; (d) the PD of Zein NPs using a syringe pump synthesis under standard conditions with stabilizers (0.5% TW80 1.0% P-F68), $n = 9$; (e) the diameter of Zein NPs using a syringe pump synthesis under standard conditions other than relative flow rate (RFR) [RFR 1:5], $n = 27$; (f) the PD of Zein NPs using a syringe pump synthesis under standard conditions other than RFR [RFR 1:5], $n = 27$; (g) the diameter of Zein NPs using a syringe pump synthesis under standard conditions other than RFR [RFR 1:5] with stabilizers (0.5% TW80 1.0% PF-68), $n = 9$; (h) the PD of Zein NPs using a syringe pump synthesis under standard conditions other than RFR [RFR 1:5] with stabilizers (0.5% TW80 1.0% P-F68), $n = 9$; (i) the diameter of Zein NPs using a batch synthesis method, $n = 2$; (j) the PD of Zein NPs using a batch synthesis method, $n = 2$; (k) the diameter of Zein NPs using a syringe pump synthesis with a T-Junction under standard conditions, $n = 9$; and (l) the PD of Zein NPs using a syringe pump synthesis with a T-Junction under standard conditions, $n = 9$.

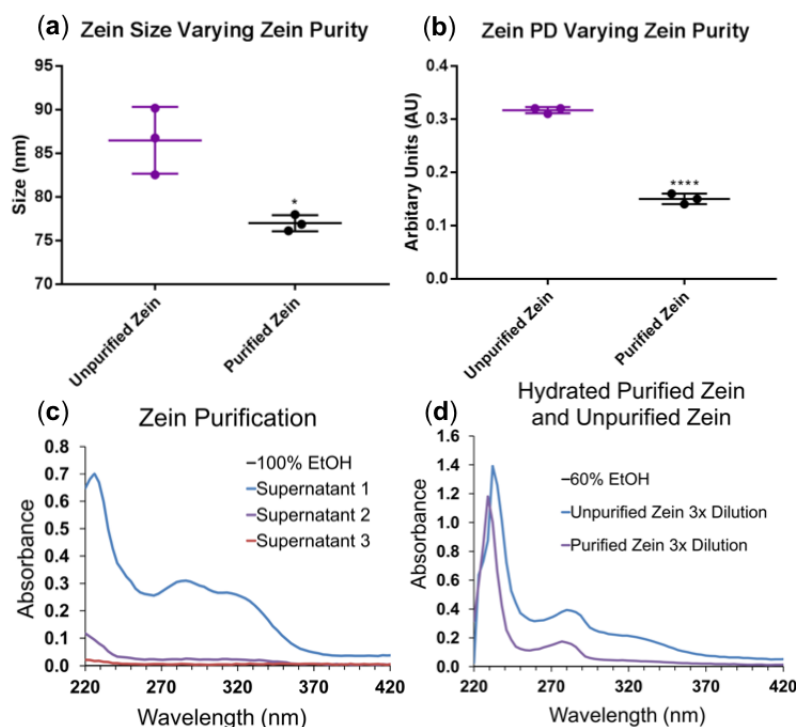


Figure A4. (a) The diameter of Zein nanoparticles' (NPs') varying purities; (b) The polydispersity (PD) of Zein NPs' varying purity; (c) the Ultraviolet-Visible Spectroscopy (UV-Vis) of each of the supernatants used to purify the Zein; (d) UV-Vis of a 3x dilution 1% unpurified Zein stock relative to a 3x dilution 1% purified Zein stock.

Zein contains removable, colored impurities, such as xanthophylls (including lutein, zeaxanthin, and β -cryptoxanthin) and β -carotene [28,48]. The presence of these impurities has been known to increase the polydispersity of Zein NPs and decrease their drug encapsulation efficiency; therefore, it can be understood why there have been increasingly more efforts put into purifying Zein [28,48,50]. To remove the impurities in our studies, the Zein powder from the manufacturer was washed using 100% ethanol, in which the Zein does not dissolve, but the impurities do. The number of washing steps necessary was determined by collecting the supernatants of three consecutive washes and measuring their absorption spectra (Figure A4c). The results indicate that one washing step was sufficient to remove most impurities from the Zein. Similar results were shown by De Boer et al. [28]. To verify that the colored impurities were removed, the absorption spectra of the diluted unpurified and purified Zein solutions were compared using UV-Vis (Figure A4d). After purification, a lower absorption is observed in the wavelength range of 220 to 420 nm than for the unpurified Zein. Based on the absorbance of the collected supernatants, this suggests that most of the impurities were successfully removed. These purified and unpurified Zein solutions were then used with the microfluidics chip under standard conditions (1.00% *w/v* Zein stock solution, an ethanol concentration 60% *v/v*, a relative flow rate (aqueous to organic phase) fixed at 3 to 1, and a total flow rate of 2.00 mL/min). As seen in Figure A4a, the size variability between batches using purified Zein was much less than those of the unpurified Zein. Additionally, as seen in Figure A4b, the PD of the purified Zein NPs was significantly more monodisperse than the unpurified Zein NPs. These findings suggest that a Y-channel microfluidics chip could be a suitable candidate in producing small, monodisperse Zein NPs for pharmaceutical applications, such as drug delivery.

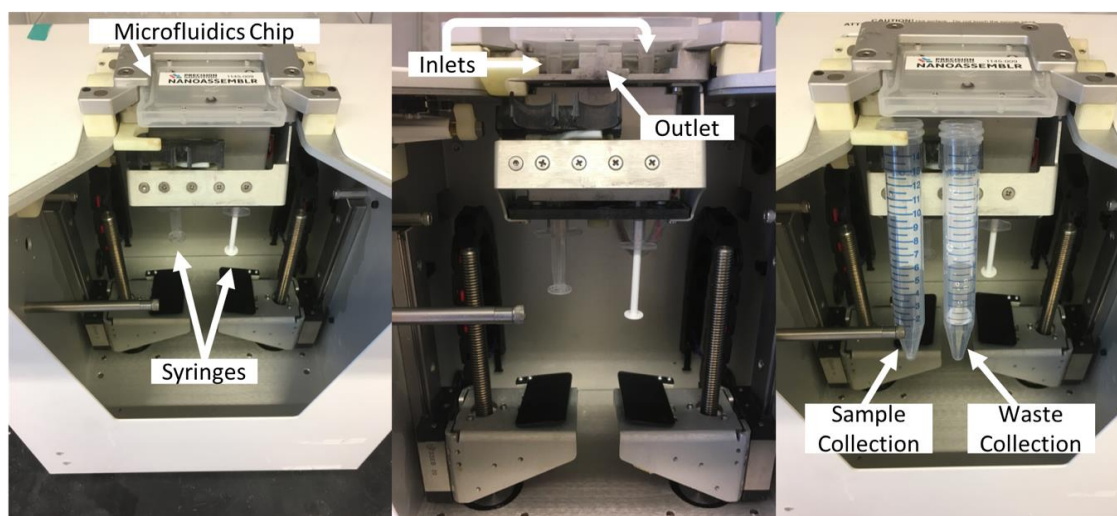


Figure A5. Depiction of the microfluidics device, NanoAssemblr, and its major components.

References

1. Karve, S.; Werner, M.E.; Li, C.; Sukumar, R.; Cummings, N.D.; Copp, J.A.; Wang, E.C.; Sethi, M.; Chen, R.C.; Pacold, M.E.; et al. Revival of the Abandoned Therapeutic Wortmannin by Nanoparticle Drug Delivery. *Proc. Natl. Acad. Sci. USA* **2012**, *109*, 8230–8235. [[CrossRef](#)] [[PubMed](#)]
2. Wicki, A.; Witzigmann, D.; Balasubramanian, V.; Huwyler, J. Nanomed. in Cancer Therapy: Challenges, Opportunities, and Clinical Applications. *J. Control. Release* **2015**, *200*, 138–157. [[CrossRef](#)] [[PubMed](#)]
3. Hobbs, S.K.; Monsky, W.L.; Yuan, F.; Roberts, W.G.; Griffith, L.; Torchilin, V.P.; Jain, R.K. Regulation of Transport Pathways in Tumor Vessels: Role of Tumor Type and Microenvironment. *Proc. Natl. Acad. Sci. USA* **1998**, *95*, 4607–4612. [[CrossRef](#)]
4. Golden, P.L.; Huwyler, J.; Pardridge, W.M. Treatment of Large Solid Tumors in Mice with Daunomycin-Loaded Sterically Stabilized Liposomes. *Drug Deliv.* **1998**, *5*, 207–212. [[CrossRef](#)] [[PubMed](#)]
5. Gelderblom, H.; Verweij, J.; Nooter, K.; Sparreboom, A. Cremophor EL: The Drawbacks and Advantages of Vehicle Selection for Drug Formulation. *Eur. J. Cancer* **2001**, *37*, 1590–1598. [[CrossRef](#)]
6. Schroeder, A.; Honen, R.; Turjeman, K.; Gabizon, A.; Kost, J.; Barenholz, Y. Ultrasound Triggered Release of Cisplatin from Liposomes in Murine Tumors. *J. Control. Release* **2009**, *137*, 63–68. [[CrossRef](#)] [[PubMed](#)]
7. van Ballegooye, C.; Man, A.; Win, M.; Yapp, D. Spatially Specific Liposomal Cancer Therapy Triggered by Clinical External Sources of Energy. *Pharmaceutics* **2019**, *11*, 125. [[CrossRef](#)]
8. Yang, X.; Yang, S.; Chai, H.; Yang, Z.; Lee, R.J.; Liao, W.; Teng, L. A Novel Isoquinoline Derivative Anticancer Agent and Its Targeted Delivery to Tumor Cells Using Transferrin-Conjugated Liposomes. *PLoS ONE* **2015**, *10*, e0136649. [[CrossRef](#)]
9. Jahanshahi, M.; Babaei, Z. Protein Nanoparticle: A Unique Wywtem as Drug Delivery Vehicles. *Afr. J. Biotechnol.* **2008**, *7*, 4926–4934. [[CrossRef](#)]
10. Weber, C.; Coester, C.; Kreuter, J.; Langer, K. Desolvation Process and Surface Characterisation of Protein Nanoparticles. *Int. J. Pharm.* **2000**, *194*, 91–102. [[CrossRef](#)]
11. Du, J.; Du, X.; Mao, C.; Wang, J. Tailor-Made Dual PH-Sensitive Polymer A Doxorubicin Nanoparticles. *J. Am. Chem. Soc.* **2011**, *133*, 17560–17563. [[CrossRef](#)] [[PubMed](#)]
12. Reddy, N.; Yang, Y. Potential of Plant Proteins for Medical Applications. *Trends Biotechnol.* **2011**, *29*, 490–498. [[CrossRef](#)]
13. Bowes, J.H.; Elliott, R.G.; Moss, J.A. The Composition of Collagen and Acid-Soluble Collagen of Bovine Skin. *Biochem. J.* **1955**, *61*, 143–150. [[CrossRef](#)] [[PubMed](#)]
14. Sen, K.; Babu, K.M. Studies on Indian Silk. I. Macrocharacterization and Analysis of Amino Acid Composition. *J. Appl. Polym. Sci.* **2004**, *92*, 1080–1097. [[CrossRef](#)]

15. Rombouts, I.; Lamberts, L.; Celus, I.; Lagrain, B.; Brijs, K.; Delcour, J.A. Wheat Gluten Amino Acid Composition Analysis by High-Performance Anion-Exchange Chromatography with Integrated Pulsed Amperometric Detection. *J. Chromatogr. A* **2009**, *1216*, 5557–5562. [\[CrossRef\]](#)
16. Yardley, D.A. Nab-Paclitaxel Mechanisms of Action and Delivery. *J. Control. Release* **2013**, *170*, 365–372. [\[CrossRef\]](#)
17. Elzoghby, A.O.; Samy, W.M.; Elgindy, N.A. Albumin-Based Nanoparticles as Potential Controlled Release Drug Delivery Systems. *J. Control. Release* **2012**, *157*, 168–182. [\[CrossRef\]](#)
18. Li, K.-K.; Yin, S.-W.; Yin, Y.-C.; Tang, C.-H.; Yang, X.-Q.; Wen, S.-H. Preparation of Water-Soluble Antimicrobial Zein Nanoparticles by a Modified Antisolvent Approach and Their Characterization. *J. Food Eng.* **2013**, *119*, 343–352. [\[CrossRef\]](#)
19. Shukla, R.; Cheryan, M. Zein: Industrial Protein from Corn. *Ind. Crops Prod.* **2001**, *13*, 171–192. [\[CrossRef\]](#)
20. Zhong, Q.; Jin, M. Zein Nanoparticles Produced by Liquid-Liquid Dispersion. *Food Hydrocoll.* **2009**, *23*, 2380–2387. [\[CrossRef\]](#)
21. Zou, T.; Li, Z.; Percival, S.S.; Bonard, S.; Gu, L. Fabrication, Characterization, and Cytotoxicity Evaluation of Cranberry Procyanidins-Zein Nanoparticles. *Food Hydrocoll.* **2012**, *27*, 293–300. [\[CrossRef\]](#)
22. Bai, G.; Bee, J.S.; Biddelcombe, J.G.; Chen, Q.; Leach, W.T. Computational Fluid Dynamics (CFD) Insights into Agitation Stress Methods in Biopharmaceutical Development. *Int. J. Pharm.* **2012**, *423*, 264–280. [\[CrossRef\]](#) [\[PubMed\]](#)
23. DeMello, J.; DeMello, A. Microscale Reactors: Nanoscale Products. *Lab Chip* **2004**, *4*, 11–15. [\[CrossRef\]](#)
24. Karnik, R.; Gu, F.; Basto, P.; Cannizzaro, C.; Dean, L.; Kyei-Manu, W.; Langer, R.; Farokhzad, O.C. Microfluidic Platform for Controlled Synthesis of Polymeric Nanoparticles. *Nano Lett.* **2008**, *8*, 2906–2912. [\[CrossRef\]](#) [\[PubMed\]](#)
25. Teh, S.Y.; Lin, R.; Hung, L.H.; Lee, A.P. Droplet Microfluidics. *Lab Chip* **2008**, *8*, 198–220. [\[CrossRef\]](#) [\[PubMed\]](#)
26. Maan, A.A.; Schroën, K.; Boom, R.; Khan, M.K.I.; Nazir, A. Microfluidic Emulsification in Food Processing. *J. Food Eng.* **2015**, *147*, 1–7. [\[CrossRef\]](#)
27. Baars, R.J.; van Leeuwen, Y.M.; Hendrix, Y.; Velikov, K.P.; Kegel, W.K.; Philipse, A.P. Morphology Controlled Functional Colloids by Heterocoagulation of Zein and Nanoparticles. *Coll. Surf. A Physicochem. Eng. Asp.* **2015**, *483*, 209–215. [\[CrossRef\]](#)
28. De Boer, F.Y.; Kok, R.N.U.; Imhof, A.; Velikov, K.P. White Zein Colloidal Particles: Synthesis and Characterization of Their Optical Properties on the Single Particle Level and in Concentrated Suspensions. *Soft Matter* **2018**. [\[CrossRef\]](#)
29. Patel, A.; Hu, Y.; Tiwari, J.K.; Velikov, K.P. Synthesis and Characterisation of Zein-Curcumin Colloidal Particles. *Soft Matter* **2010**, *6*, 6192–6199. [\[CrossRef\]](#)
30. Vitale, S.A.; Katz, J.L. Liquid Droplet Dispersions Formed by Homogeneous Liquid–Liquid Nucleation: “The Ouzo Effect”. *Langmuir* **2003**, *19*, 4105–4110. [\[CrossRef\]](#)
31. Olenskyj, A.G.; Feng, Y.; Lee, Y. Continuous Microfluidic Production of Zein Nanoparticles and Correlation of Particle Size with Physical Parameters Determined Using CFD Simulation. *J. Food Eng.* **2017**, *211*, 50–59. [\[CrossRef\]](#)
32. Li, F.; Chen, Y.; Shubo, L.; Qi, J.; Wang, W.; Wang, C.; Zhong, R.; Cheng, Z.; Li, X.; Guan, Y.; et al. Size-controlled fabrication of zein nano/microparticles by modified anti-solvent precipitation with/without sodium caseinate. *Int. J. Nanomed.* **2017**, *12*, 8197–8209. [\[CrossRef\]](#)
33. Kim, S.; Xu, J. Aggregate formation of zein and its structural inversion in aqueous ethanol. *J. Cereal Sci.* **2008**, *47*, 1–5. [\[CrossRef\]](#)
34. Rossi, L.; Seijen Ten Hoorn, J.W.M.; Melnikov, S.M.; Velikov, K.P. Colloidal Phytosterols: Synthesis, Characterization and Bioaccessibility. *Soft Matter* **2010**, *6*, 928–936. [\[CrossRef\]](#)
35. Kyte, J.; Doolittle, R.F.J. A simple method for displaying the hydropathic character of a protein. *J. Mol. Biol.* **1982**, *157*, 105–132. [\[CrossRef\]](#)
36. Li, Y.; Li, J.; Xia, Q.; Zhang, B.; Wang, Q.; Huang, Q. Understanding the Dissolution of α -Zein in Aqueous Ethanol and Acetic Acid Solutions. *J. Phys. Chem. B* **2012**, *116*, 12057–12064. [\[CrossRef\]](#)
37. Schwarzenbach, R.P.; Gschwend, P.M.; Imboden, D.M. *Environmental Organic Chemistry*, 2nd ed.; John Wiley & Sons, Inc.: Hoboken, NJ, USA, 2003; pp. 1191–1208.
38. Moldoveanu, S.C.; David, V. *Solvents, Buffers, and Additives Used in the Mobile Phase*; Elsevier Inc.: Amsterdam, The Netherlands, 2017. [\[CrossRef\]](#)

39. Hao, L.; Leaist, D.G. Binary Mutual Diffusion Coefficients of Aqueous Alcohols. Methanol to 1-Heptanol. *J. Chem. Eng. Data* **1996**, *41*, 210–213. [[CrossRef](#)]
40. Zhu, Q.; Moggridge, G.D.; D'Agostino, C. A Local Composition Model for the Prediction of Mutual Diffusion Coefficients in Binary Liquid Mixtures from Tracer Diffusion Coefficients. *Chem. Eng. Sci.* **2015**, *132*, 250–258. [[CrossRef](#)]
41. Cheng, D.; Yong, X.; Zhu, T.; Qiu, Y.; Wang, J.; Zhu, H.; Ma, B.; Xie, J. Synthesis of Protein Nanoparticles for Drug Delivery. *Eur. J. Biomed. Res.* **2016**, *2*, 8–11. [[CrossRef](#)]
42. Hu, K.; McClements, D. Fabrication of biopolymer nanoparticles by antisolvent precipitation and electrostatic deposition: Zein-alginate core/shell nanoparticles. *Food Hydrocoll.* **2015**, *44*, 101–108. [[CrossRef](#)]
43. Hu, K.; McClements, D. Fabrication of surfactant-stabilized zein nanoparticles: A pH modulated antisolvent precipitation method. *Food Res. Int.* **2014**, *64*, 229–235. [[CrossRef](#)] [[PubMed](#)]
44. Luo, Y.; Teng, Z.; Wang, T.T.Y.; Wang, Q. Cellular Uptake and Transport of Zein Nanoparticles: Effects of Sodium Caseinate. *J. Agric. Food Chem.* **2013**, *61*, 7621–7629. [[CrossRef](#)] [[PubMed](#)]
45. Jain, A.; Sharma, G.; Kushwah, V.; Ghoshal, G.; Jain, A.; Singh, B.; Shivhare, U.S.; Jain, S.; Katare, O.P. Beta Carotene-Loaded Zein Nanoparticles to Improve the Biopharmaceutical Attributes and to Abolish the Toxicity of Methotrexate: A Preclinical Study for Breast Cancer. *Artif. Cells Nanomed. Biotechnol.* **2018**, *46*, 402–412. [[CrossRef](#)] [[PubMed](#)]
46. Elzoghby, A.O.; Helmy, M.W.; Samy, W.M.; Elgindy, N.A. Novel Ionically Crosslinked Casein Nanoparticles for Flutamide Delivery: Formulation, Characterization, and in Vivo Pharmacokinetics. *Int. J. Nanomed.* **2013**, *8*, 1721–1732. [[CrossRef](#)]
47. Mahal, A.; Khullar, P.; Kumar, H.; Kaur, G.; Singh, N.; Jelokhani-Niaraki, M.; Bakshi, M.S. Green Chemistry of Zein Protein toward the Synthesis of Bioconjugated Nanoparticles: Understanding Unfolding, Fusogenic Behavior, and Hemolysis. *ACS Sustain. Chem. Eng.* **2013**, *1*, 627–639. [[CrossRef](#)]
48. Podaralla, S.; Perumal, O. Influence of Formulation Factors on the Preparation of Zein Nanoparticles. *AAPS PharmSciTech* **2012**, *13*, 919–927. [[CrossRef](#)] [[PubMed](#)]
49. Thapa, R.K.; Nguyen, H.T.; Jeong, J.H.; Shin, B.S.; Ku, S.K.; Choi, H.G.; Yong, C.S.; Kim, J.O. Synergistic Anticancer Activity of Combined Histone Deacetylase and Proteasomal Inhibitor-Loaded Zein Nanoparticles in Metastatic Prostate Cancers. *Nanomed. Nanotechnol. Biol. Med.* **2016**, *13*, 885–896. [[CrossRef](#)] [[PubMed](#)]
50. Elzoghby, A.; Freag, M.; Mamdouh, H.; Elkhodairy, K. Zein-based Nanocarriers as Potential Natural Alternatives for Drug and Gene Delivery: Focus on Cancer Therapy. *Curr. Pharm. Des.* **2017**, *23*, 5261–5271. [[CrossRef](#)]



© 2019 by the authors. Licensee MDPI, Basel, Switzerland. This article is an open access article distributed under the terms and conditions of the Creative Commons Attribution (CC BY) license (<http://creativecommons.org/licenses/by/4.0/>).